

Anomalous Dispersion of Longitudinal Optical Phonons in $\text{Nd}_{1.86}\text{Ce}_{0.14}\text{CuO}_{4+\delta}$ Determined by Inelastic X-ray Scattering

M. d'Astuto,¹ P. K. Mang,² P. Giura,¹ A. Shukla,¹ P. Ghigna,³
A. Mirone,¹ M. Braden,⁴ M. Greven,^{2,5} M. Krisch,¹ and F. Sette¹

¹European Synchrotron Radiation Facility, BP 220, F-38043 Grenoble Cedex, France

²Department of Applied Physics, Stanford University, Stanford, California 94305

³Dipartimento di Chimica Fisica "M. Rolla", Un. Pavia, V.le Taramelli 16, I-27100, Pavia, Italy

⁴II. Physikalisches Inst., Univ. zu Köln, Zùlpicher Str. 77, 50397 Köln, Germany

⁵Stanford Synchrotron Radiation Laboratory, Stanford, California 94305

(Dated: March 22, 2022)

The phonon dispersions of $\text{Nd}_{1.86}\text{Ce}_{0.14}\text{CuO}_{4+\delta}$ along the $[\xi, 0, 0]$ direction have been determined by inelastic x-ray scattering. Compared to the undoped parent compound, the two highest longitudinal phonon branches, associated with the Cu-O bond-stretching and out-of-plane oxygen vibration, are shifted to lower energies. Moreover, an anomalous softening of the bond-stretching band is observed around $\mathbf{q} = (0.2, 0, 0)$. These signatures provide evidence for strong electron-phonon coupling in this electron-doped high-temperature superconductor.

While the coupling between electrons and phonons is known to be the driving mechanism for Cooper-pair formation in conventional superconductors, its role in the high-critical-temperature superconductors (HTcS) is the subject of intense research efforts. Recently, evidence for electron-phonon coupling has been invoked in the interpretation of inelastic neutron scattering (INS) and angle-resolved photoemission spectroscopy (ARPES) experiments. The INS studies, carried out on $\text{La}_{1.85}\text{Sr}_{0.15}\text{CuO}_{4+\delta}$ [1, 2, 3, 4], oxygen-doped $\text{La}_2\text{CuO}_{4+\delta}$ [5] and $\text{YBa}_2\text{Cu}_3\text{O}_{6+\delta}$ [2, 6] reveal an anomalous softening with doping of the highest longitudinal optical (LO) phonon branch, in particular along the $q = [\xi, 0, 0]$ direction. This branch is assigned to the Cu-O bond-stretching mode [2, 7]. The observed softening has been interpreted as a signature of a strong electron-phonon coupling [2, 3], which has been discussed since the discovery of HTcS [8, 9]. Furthermore, in an energy range similar to the LO bond-stretching phonon band, ARPES studies on three different families of hole-doped HTcS reveal a distinct "kink" anomaly in the quasiparticle dispersion [10]. The scenario emerging from the above INS and ARPES works suggests a strong coupling between the charge carriers and the Cu-O bond-stretching phonon modes to be ubiquitous in HTcS materials, at least for hole-doped compounds. However, its role in the pairing mechanism remains completely unclear [4]. At the moment, it may not even be excluded that the electron-phonon interaction is pair-breaking for the d-wave superconducting order parameter. Therefore, it appears very important to analyze the strength of the phonon anomalies in as many cuprate families as possible and to compare them with their superconducting properties. In this context, the electron-doped cuprates are of central importance due to the distinct character of the doped charges in this material: Cu $3d_{x^2-y^2}$ (O $2p$) for n(p)-type cuprates [11], leading to a very different electronic structure [12]. Since the phonon anomalies are related

to a coupling between charge fluctuations and phonons, charges with different character may induce quite different electron-phonon interactions.

In this Letter, we present an inelastic x-ray scattering (IXS) study of the phonon dispersion in the n-type cuprates $\text{Nd}_{1.86}\text{Ce}_{0.14}\text{CuO}_{4+\delta}$ (NCCO). Inelastic x-ray scattering can overcome the main limitation of inelastic neutron scattering, *i.e.* the need for sufficiently large single crystals of high chemical and structural quality [2]. Lateral x-ray beam sizes of few tens of μm are routinely obtained. Moreover, at photon energies around 10-20 keV and $Z > 3$, the total cross section is dominated by photoelectric absorption, and therefore the typical x-ray penetration depths for high- Z materials is of the order of 10 - 100 μm . Consequently, very small samples (down to less than 10^{-4} mm^3) can be studied with signal rates comparable to typical INS experiments on cm^3 -sized samples. Despite these advantages, little work has been done using IXS on the HTcS compounds [13]. We choose $\text{Nd}_{2-x}\text{Ce}_x\text{CuO}_{4+\delta}$ for our IXS study, since its crystallographic structure is one of the simplest among the HTcS, and because extensive INS studies exist for its undoped parent compound $\text{Nd}_2\text{CuO}_{4+\delta}$ (NCO) [1, 2]. Our interest is focused on the $[\xi, 0, 0]$ direction, where the LO branch displays its strongest anomaly for hole-doped HTcS [3, 4]. The present results reveal that, near the zone center, the two highest longitudinal optical branches, assigned to the Cu-O bond-stretching and O(2) vibration modes, are shifted to lower frequencies with respect to the undoped parent compound. The interpretation of our data is supported by lattice dynamics calculations, taking into account a *Thomas-Fermi* screening mechanism. Furthermore, we observe an anomalous softening of the highest branch around $\mathbf{q} = (0.2, 0, 0)$. Our results demonstrate that this anomalous behavior of the high-energy LO phonon branch is a universal property of both hole- and electron-doped HTcS compounds, therefore providing further evidence that electron-phonon in-

teractions may play an important role in high- T_c superconductivity. Furthermore, the present results are an important demonstration of IXS as a powerful tool for the study of the lattice dynamics in small, high-quality crystals of complex transition metal oxides.

The experiment was carried out at the very-high-energy-resolution IXS beam-line ID16 at the European Synchrotron Radiation Facility (ESRF). X-rays from an undulator source were monochromated using a Si (111) double-crystal monochromator, followed by a high-energy-resolution backscattering monochromator [14], operating at 15816 eV (Si (888) reflection order). A toroidal gold-coated mirror refocused the x-ray beam onto the sample, where a beam size of $250 \times 250 \mu\text{m}^2$ full-width-half-maximum (FWHM) was obtained. The scattered photons were energy-analyzed by a spherical silicon crystal analyzer 3 m in radius, operating at the same Bragg reflection as the monochromator [15]. The total energy resolution was 1.6 THz (6.6 meV) FWHM. The momentum transfer \mathbf{Q} was selected by rotating the 3 m spectrometer arm in the scattering plane perpendicular to the linear x-ray polarization vector of the incident beam. The momentum resolution was set to $\approx 0.087 \text{ \AA}^{-1}$ in both the horizontal and the vertical direction by an aperture of $20 \times 20 \text{ mm}^2$ in front of the analyzer. Further experimental details are given elsewhere ([14, 15] and references therein). The sample is a single crystal grown by the traveling-solvent floating-zone method in 4 atm of O_2 at Stanford University. It has been reduced under pure Ar atmosphere at 920°C for 20 h, followed by a further 20 h of exposure at 500°C to a pure O_2 atmosphere. Such a procedure is necessary to produce a superconducting phase in $\text{Nd}_{1.86}\text{Ce}_{0.14}\text{CuO}_{4+\delta}$, although its exact effect is not understood. Following this treatment the sample had a narrow superconducting transition with an onset temperature of $T_c = 24 \text{ K}$. The sample is of very good crystalline quality, with a rocking curve width of 0.02° (FWHM) around the $[h, 0, 0]$ direction. It was mounted on the cold finger of a closed-loop helium cryostat, and cooled to 15 K. The experiment was performed in reflection geometry, and the probed scattering volume corresponded to about $1.5 \times 10^{-3} \text{ mm}^3$. IXS scans were performed in the $-2 < \nu < 24 \text{ THz}$ range, in the $\tau = (6, 0, 0)$ and $\tau = (7, 1, 0)$ Brillouin zones [18]. The data were collected along the following three lines: I) $\mathbf{Q} = (6 + \xi, 0, 0)$, in longitudinal configuration (*i.e.* with $\mathbf{q} = (\xi, 0, 0) \parallel \mathbf{Q}$), II) $\mathbf{Q} = (7 \pm \xi, 1, 0)$ in almost longitudinal configuration (*i.e.* with $\mathbf{q} = (\xi, 0, 0)$ and $(\mathbf{Q} \cdot \mathbf{q})/Q \approx q$), III) $\mathbf{Q} = (7, 1 - \xi, 0)$ in almost transverse configuration ($\mathbf{q} = (0, \xi, 0)$ and $(\mathbf{Q} \cdot \mathbf{q})/Q \approx 0$). The low temperature and high momentum transfer were chosen so as to optimize the count rate on the high-frequency optical mode while limiting the loss of contrast due to the contribution from the tails of the intense low frequency acoustic modes.

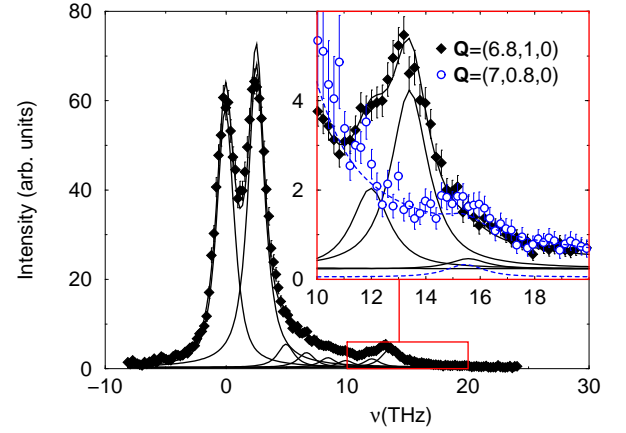


FIG. 1: Experimental IXS phonon spectra of $\text{Nd}_{1.86}\text{Ce}_{0.14}\text{CuO}_{4+\delta}$ at $T = 15 \text{ K}$ and corresponding harmonic oscillator model best fits (solid and dotted lines). Both scans were performed in the $\tau = (7, 1, 0)$ Brillouin zones with a propagation vector of $\xi = 0.2$ in an almost longitudinal geometry along the a^* direction (diamonds) and in an almost transverse geometry along b^* (open circles).

Fig. 1 shows a typical energy scan in almost longitudinal geometry at $\mathbf{Q} = (6.8, 1, 0)$, corresponding to $\xi = 0.2$. The data are shown together with the results of a fit, where the excitations were modeled by harmonic oscillators, convoluted with the instrumental resolution function. Three features can be clearly distinguished: (i) an elastic peak at 0 THz, due to chemical disorder and, possibly, strain due to the different thermal expansion coefficients between the sample and the sample support during cooling, (ii) the longitudinal acoustic phonon, centered near 2.7 THz and (iii) a weaker feature around 13 THz. In the intermediate energy region (from about 4 to 10 THz), no distinct phonon peaks are resolved due to the dominating contribution from the tails of the elastic and acoustic phonon signals. The inset of Fig. 1 emphasizes the high-energy region of the spectrum. One can clearly distinguish two phonons, centered around 12 and 13.5 THz, respectively. The weak shoulder at around 16 THz can be attributed to an admixture of the transverse optical (TO) mode, as indicated by the comparison (after normalization to the same intensity at 20 THz) with the equivalent scan in transverse geometry $\mathbf{Q} = (7, 0.8, 0)$. Consequently, the two stronger peaks are unambiguously assigned to longitudinal optical (LO) modes. From the absence of other higher frequency modes up to 23 THz, we conclude that the two modes at 12 and 13.5 THz can be identified with the O(2) vibration and Cu-O bond-stretching modes, respectively (see Refs. 2, 7).

In order to determine the dispersion of the two highest LO branches, IXS spectra were recorded for $0 < \xi \leq 1$. In Fig. 2 we show three spectra taken along the $(7 - \xi, 1, 0)$ direction. Close to the zone center, at $\mathbf{q} = (0.1, 0, 0)$, the highest frequency mode is observed slightly above 15

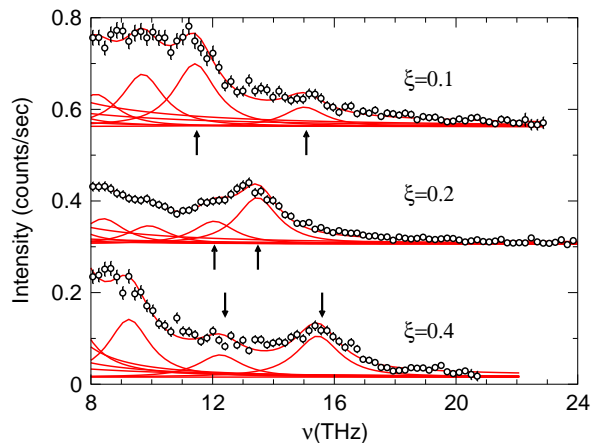


FIG. 2: IXS spectra in the $\tau = (7, 1, 0)$ Brillouin zone with propagation vector \mathbf{q} along a^* , as indicated in the figure. The experimental data (circles) are shown together with their corresponding harmonic oscillator model best fits (solid lines), as discussed in the text.

THz. At $\mathbf{q} = (0.2, 0, 0)$ the highest mode is found at the much lower energy of 13.5 THz. Finally, for $\mathbf{q} = (0.4, 0, 0)$, we again find a high-frequency mode around 15.5 THz.

The peak positions extracted from these and many other scans are summarized in Fig. 3. The highest branch exhibits a sharp dip around $\mathbf{q} = (0.2, 0, 0)$ and recovers for larger q -values. This behavior is most likely due to an anti-crossing with the second highest branch which is mainly associated with vibrations of the O(2) position in the ξ -direction. Therefore, within a standard anti-crossing framework, one should interpret the highest longitudinal intensities for $\mathbf{q} = (0.3, 0, 0)$ and above as being mainly due to O(2) vibration. Within that scenario, this second-highest branch increases its frequency in the middle of the zone as in the undoped compound, and, except for the fact that the *Lyddane-Sachs-Teller* (LO-TO) gap closes, seems to be insensitive to doping. The LO bond-stretching mode just above $\mathbf{q} = (0.2, 0, 0)$ is then found at quite low energies, ~ 12 THz, but can not be unambiguously followed to larger q -values. Nevertheless, our data document that the LO bond-stretching branch in NCCO is strongly renormalized compared to undoped NCO, in particular it bends down anomalously from the zone center to $\mathbf{q} = (0.2, 0, 0)$.

In order to further validate the correctness of our assignments, we performed a lattice dynamical calculation [16] based on a shell model. We used a common potential model for cuprates, in which the interatomic potentials have been derived from a comparison of INS results for different HTcS compounds by Chaplot *et al.* [17], using a screened Coulomb potential, in order to simulate the effect of the free carriers introduced by doping. Following Ref. [17] for metallic $\text{La}_{1.85}\text{Sr}_{0.15}\text{CuO}_{4+\delta}$ and $\text{YBa}_2\text{Cu}_3\text{O}_7$, we replaced the long-range Coulomb po-

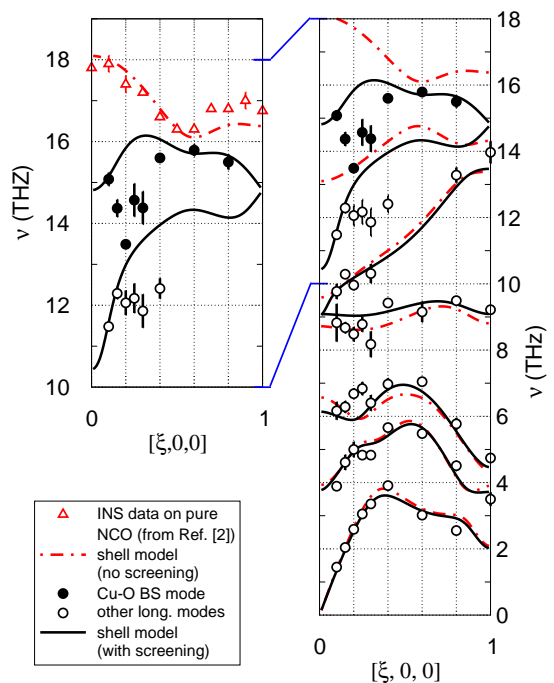


FIG. 3: Right hand side: (o, •) experimental longitudinal phonon frequencies determined from IXS spectra in NCCO at $T = 15$ K along the $[\xi, 0, 0]$ direction. Solid circles (•) emphasize the highest energy frequencies measured. Solid (dot-dashed) lines indicate lattice dynamics calculation with a screened (unscreened) Coulomb interaction. Left hand side: magnification of the high energy portion of the right hand side graph showing the dispersion of the top two phonon branches. The highest frequency parent (Δ), as measured by INS (from Ref. [1]) in the insulating parent compound $\text{Nd}_2\text{CuO}_{4+\delta}$ is shown for comparison. The experimental data are in agreement with calculations, except for the anomalous softening at $q = (0.2, 0, 0)$ of the two higher energy branches (see text).

tential $V_c(q)$ by $V_c(q)/\epsilon(q)$, and for the dielectric function we take the semi-classical *Thomas-Fermi* limit of $\epsilon(q) = 1 + \kappa_s^2/q^2$, where κ_s^2 indicates the screening vector. The results of the calculation (without screening: dot-dashed lines; with screening: solid lines) are shown as well in Fig. 3. The lattice dynamics calculations without screening have been included, since they reproduce very well the experimental dispersion of the undoped parent compound [1]. The shift at the zone center of the high-energy phonon branches of NCCO with respect to NCO is due to the closing of a large LO-TO splitting. Indeed, the corresponding Δ_1 and Δ_3 branches in $\text{Nd}_2\text{CuO}_{4+\delta}$ are separated by almost 3 THz at the zone center, as observed by INS [1]. We point out that in our case a strong softening due to *Thomas-Fermi* screening does not imply a higher *Thomas-Fermi* parameter κ_s : actually, we find a screening vector κ_s of about 0.39 \AA^{-1} , which is comparable to that for $\text{La}_{1.85}\text{Sr}_{0.15}\text{CuO}_{4+\delta}$ [17]. Though our modified calculation reproduces the closing of the LO-

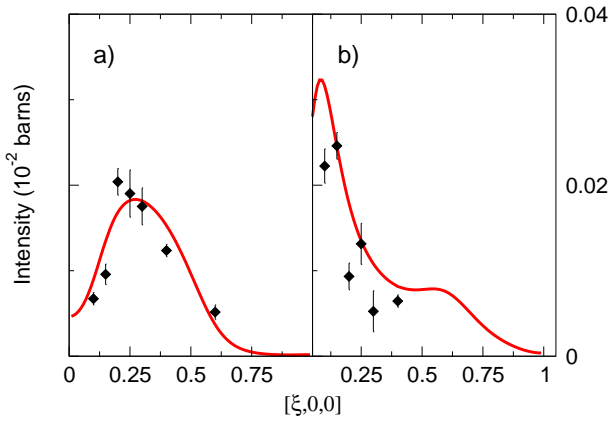


FIG. 4: Comparison between experimental (diamonds) and calculated (line) phonon intensities for the two highest optical phonon branches along $(7 - \xi, 1, 0)$. a) bond-stretching LO mode starting around 15 THz and b) O(2) vibration LO branch starting around 10.5 THz.

TO splitting, we still observe an anomalous additional softening of the highest bond-stretching LO branch near $\mathbf{q} = (0.2, 0, 0)$, which is not reproduced by our calculations (see Fig. 3). This branch softens in frequency from $\mathbf{q} = (0.1, 0, 0)$ to $\mathbf{q} = (0.2, 0, 0)$ by about $\Delta\nu \approx 1.5$ THz, which is a shift comparable to the anomalous shift observed in $\text{La}_{1.85}\text{Sr}_{0.15}\text{CuO}_{4+\delta}$ at slightly larger \mathbf{q} [1, 3, 4]. Therefore, we believe that this anomalous softening is of the same nature as the one observed in p-type $\text{La}_{1.85}\text{Sr}_{0.15}\text{CuO}_{4+\delta}$.

A comparison between the experimental and calculated intensities for the two highest phonon branches is shown in Fig. 4. The good agreement of the observed integrated intensities with the calculated ones for the upper branches validates the correctness of our phonon branch assignment, at least for $\xi \leq 0.2$. For $\xi > 0.2$ we would have expected an intensity exchange between the two highest branches, which seems to be not observed.

The main difference between $\text{La}_{1.85}\text{Sr}_{0.15}\text{CuO}_{4+\delta}$ and $\text{Nd}_{1.86}\text{Ce}_{0.14}\text{CuO}_{4+\delta}$ is, besides the screening effect, that in NCCO the Cu-O bond-stretching branch is closer in energy to the out-of-plane oxygen vibration one, having almost the same energy at $\xi = 0.2$. These two branches belong to the same symmetry and therefore cannot cross, so that for $\xi > 0.2$ softening implies interaction with the out-of-plane oxygen vibration mode with the same symmetry. In the region between $\mathbf{q} = (0.25, 0, 0)$ and $(0.3, 0, 0)$, the two modes are poorly defined in energy, which is consistent with what is observed in $\text{La}_{1.85}\text{Sr}_{0.15}\text{CuO}_{4+\delta}$ by Pintschovius and Braden [4] and McQueeney *et al.* [3] for $\xi \sim 0.25 - 0.3$. The corresponding real space periodicity of 3 to 4 unit cells may therefore be linked to the proximity to some charge instability. We remark that a reduced vector $\xi \sim 0.25 - 0.3$ approximately corresponds to the nesting vector along $[\xi 00]$ direction, as can be inferred from the ARPES data

of Ref. 12.

In conclusion, the present results reveal that the anomalous softening previously observed in hole-doped compounds [1, 2, 3, 4, 5, 6], is also present in the electron-doped cuprates. This is evidenced by the comparison of the present results on doped NCCO with the previously reported ones on pure NCO [1]. This implies that: (i) the anomaly also exists in n-type cuprates, giving strength to the hypothesis [1, 2, 3, 4, 5, 6] of an electron-phonon coupling origin of this feature; (ii) this is a generic feature of the high-temperature superconductors, as expected, if phonons are relevant to high temperature superconductivity. Moreover, this Letter demonstrates that high-energy resolution inelastic x-ray scattering has developed into an invaluable tool for the study of the lattice dynamics of complex transition metal oxides, allowing measurements on small high-quality single crystals which are inaccessible to the traditional method of inelastic neutron scattering.

We acknowledge L. Paolasini and G. Monaco for useful discussions and H. Casalta for precious help during preliminary tests. The authors are grateful to D. Gambetti, C. Henriquet and R. Verbeni for technical help, to J.-L. Hodeau for help in the crystal orientation and J. -P. Vassalli for crystal cutting. P.K.M. and M.G. are supported by the U.S. Department of Energy under Contracts No. DE-FG03-99ER45773 and No. DE-AC03-76SF00515, by NSF CAREER Award No. DMR-9985067, and by the A.P. Sloan Foundation.

-
- [1] L. Pintschovius *et al.*, *Physica B* **174**, 323 (1991).
 - [2] L. Pintschovius and W. Reichardt, in *Physical Properties of High Temperature Superconductors*, edited by D. Ginsberg (World Scientific, Singapore, 1995), p. 295.
 - [3] R. McQueeney *et al.*, *Phys. Rev. Lett.* **82**, 628 (1999).
 - [4] L. Pintschovius and M. Braden, *Phys. Rev. B* **60**, R15039 (1999).
 - [5] L. Pintschovius and M. Braden, *J. Low Temp. Phys.* **105**, 813 (1996).
 - [6] W. Reichardt, *J. Low Temp. Phys.* **105**, 807 (1996).
 - [7] J.-G. Zhang *et al.*, *Phys. Rev. B* **43**, 5389 (1991).
 - [8] J. G. Bednorz and K. A. Müller, *Z. Phys. B* **64**, 189 (1986).
 - [9] W. Weber, *Phys. Rev. Lett.* **58**, 1371 (1987).
 - [10] A. Lanzara *et al.*, *Nature* **412**, 510 (2001).
 - [11] Y. Tokura *et al.*, *Nature* **337**, 345 (1989).
 - [12] N. P. Armitage *et al.*, *Phys. Rev. Lett.* **87**, 147003 (2001).
 - [13] E. Burkel, *Inelastic Scattering of X-rays with Very High Energy Resolution* (Springer Verlag, 1991), p65, Fig. 6.9.
 - [14] R. Verbeni *et al.*, *J. Synch. Rad.* **3**, 62 (1996).
 - [15] C. Masciovecchio *et al.*, *Nucl. Inst. Methods B* **111**, 181 (1996).
 - [16] A. Mirone, *OpenPhonon code source* (2001), available on <http://www.esrf.fr/computing/scientific/>.
 - [17] S. L. Chaplot *et al.*, *Phys. Rev. B* **52**, 7230 (1995).
 - [18] All reciprocal lattice vectors are expressed in r.l.u.